



<b>Publication Year</b>	2023
<b>Acceptance in OA</b>	2024-12-20T13:39:13Z
<b>Title</b>	6.7 GHz CH <sub>3</sub> OH masers polarization in massive star-forming regions: the Flux-Limited Sample
<b>Authors</b>	Surcis, Gabriele, Vlemmings, Wouter, van Langevelde, Huib Jan, Hutawarakorn Kramer, Busaba, Bartkiewicz, Anna
<b>Handle</b>	<a href="http://hdl.handle.net/20.500.12386/35543">http://hdl.handle.net/20.500.12386/35543</a>
<b>Serie</b>	POS PROCEEDINGS OF SCIENCE
<b>Volume</b>	PoS(EVN2022)

## 6.7 GHz CH<sub>3</sub>OH masers polarization in massive star-forming regions: the Flux-Limited Sample

Gabriele Surcis,<sup>a,\*</sup> Wouter Vlemmings,<sup>b</sup> Huib Jan van Langevelde,<sup>c,d</sup> Busaba Hutawarakorn Kramer<sup>e,f</sup> and Anna Bartkiewicz<sup>g</sup>

<sup>a</sup>INAF-Osservatorio Astronomico di Cagliari,  
Via della Scienza 5, I-09047, Selargius, Italy

<sup>b</sup>Department of Space, Earth and Environment, Chalmers University of Technology,  
Onsala Space Observatory, SE-439 92 Onsala, Sweden

<sup>c</sup>Joint Institute for VLBI ERIC,  
Oude Hoogeveensedijk 4, 7991 PD Dwingeloo, The Netherlands

<sup>d</sup>Sterrewacht Leiden, Leiden University,  
Postbus 9513, 2300 RA Leiden, The Netherlands

<sup>e</sup>Max-Planck-Institut für Radioastronomie,  
Auf dem Hügel 69, 53121 Bonn, Germany

<sup>f</sup>National Astronomical Research Institute of Thailand,  
260 Moo 4, T. Donkaew, A. Maerim, Chiang Mai, 50180, Thailand

<sup>g</sup>Institute of Astronomy, Faculty of Physics, Astronomy and Informatics, Nicolaus Copernicus University,  
Grudziadzka 5, 87-100 Torun, Poland  
E-mail: [gabriele.surcis@inaf.it](mailto:gabriele.surcis@inaf.it), [wouter.vlemmings@chalmers.se](mailto:wouter.vlemmings@chalmers.se),  
[langevelde@jive.eu](mailto:langevelde@jive.eu), [bkramer@mpifr-bonn.mpg.de](mailto:bkramer@mpifr-bonn.mpg.de), [annan@astro.uni.torun.pl](mailto:annan@astro.uni.torun.pl)

The formation process of high-mass stars ( $M > 8M_{\text{sun}}$ ) is still unclear; this is mainly due to their fast evolution and large distances that make difficult to observe them in details. The observational and theoretical efforts made in the last decades have shown that a common and essential component in the formation of high-mass stars is the presence of molecular outflows during the protostellar phase, similarly to what is observed during the formation of low-mass stars. Theoretically, it has been convincingly demonstrated that the magnetic field plays an important role in launching and shaping molecular outflows in massive young stellar objects (YSOs). Therefore, providing new observational measurements of magnetic fields close (10s-100s au) to massive YSOs is of great importance. More than 10 years ago we started a large EVN campaign to measure the magnetic field orientation and strength toward a sample of 30 massive star-forming regions, called the “Flux-Limited sample”, by observing the polarized emission of 6.7 GHz CH<sub>3</sub>OH masers. Here, we present a summary of the final statistics of the Flux-Limited sample, extensively reported in [1], which are focused on the relative orientation of the outflows with the magnetic fields and on the polarized characteristics of 6.7 GHz CH<sub>3</sub>OH masers.

*15th European VLBI Network Mini-Symposium and Users' Meeting (EVN2022)*  
*11-15 July 2022*  
*University College Cork, Ireland*

---

\*Speaker

## 1. Introduction

The presence of molecular outflows during the formation process of young stellar objects (YSOs) is found to be common and essential in the whole range of masses [2–5]. In particular, magnetohydrodynamical (MHD) simulations have shown that a crucial role in the launching of molecular outflows in massive YSOs is played by the magnetic field [e.g., 6]. Besides influencing the collimation of the outflows [7, 8], the magnetic field also contributes to the formation of the so-called early outflows, which can reduce the radiation pressure significantly [9, 10]. Even though there is now consensus on the theoretical importance of magnetic fields in launching the outflows both in low- and high-mass protostellar objects, one of the still open observational issue regards the alignment of the magnetic field lines with the molecular outflows [e.g; 11]. [12] observed with the Submillimeter Array (SMA) the dust polarized emission toward a sample of 21 high-mass YSOs to measure the magnetic field orientation on scales  $> 1000$  au. The comparison between the magnetic field orientation and the outflows axis have showed that the angles formed between them show a slight preference around  $0^\circ$  and  $90^\circ$ . However, the small size of the sample made difficult to confirm at a good level of significance the bimodal distribution of the angles. Therefore, they concluded that their data were consistent with a random distribution. To provide a statistical study with a higher number of sources and with a better spatial resolution (scales  $< 100$  au), since 2008, we started to observe with the European VLBI Network<sup>1</sup> (EVN) the polarized emission of 6.7 GHz  $\text{CH}_3\text{OH}$  masers from a number of massive star-forming regions (SFRs) that in 2011 become part of the Flux-Limited sample [1, 13–19]. From these observations, it is possible to determine both the orientation and the strength of the magnetic field close to the massive YSOs. The results were presented in previous three EVN symposia (editions 2012, 2014, and 2018) and the preliminary statistical results were reported in the corresponding proceedings [20–22].

Here we present a summary of the final statistical analysis of the Flux-Limited sample, that is briefly introduced in the next section; a more detailed description can be found in [1].

## 2. The Flux-Limited Sample

In 2008 we successfully observed, for the very first time, the polarized emission of 6.7 GHz  $\text{CH}_3\text{OH}$  masers with the very long baseline interferometry (VLBI) toward the massive SFR W75N by using the EVN (pilot project code: EV017) [13]. After this pilot project, we first observed with the EVN a sample of five SFRs that host the brightest known  $\text{CH}_3\text{OH}$  maser sources (project code: ES063) [14, 15]. Thanks to the good performance of the EVN, in 2011 we decided to further select a large and complete sample of SFRs toward which the 6.7 GHz  $\text{CH}_3\text{OH}$  maser emission was detected in the past. We selected the sources from the single-dish catalog of 6.7 GHz  $\text{CH}_3\text{OH}$  masers compiled by [23]. Our first selection criterion was on the declination of the sources in order to be observed with the EVN; we selected all the sources with declination  $> -9^\circ$ . The second selection criterion was on the single-dish peak flux density of the maser emission to be able to detect the weak circularly polarized emission at significance greater than  $4\sigma$ . We first selected all the sources with single-dish flux density greater than 50 Jy, but, because the masers

<sup>1</sup>The European VLBI Network is a joint facility of European, Chinese, South African and other radio astronomy institutes funded by their national research councils.

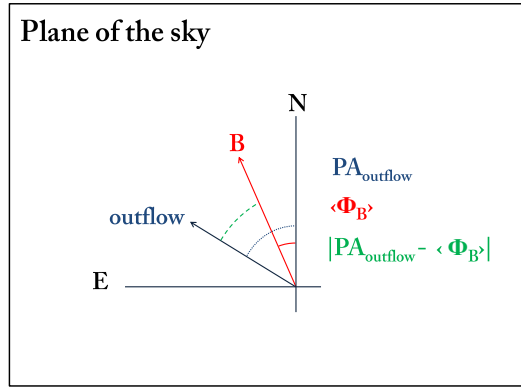


**Figure 1:** Definition of the position angle of the outflow axes ( $PA_{\text{outflow}}$ ) and of the magnetic field ( $\langle \Phi_B \rangle$ ), and of the angle between the outflow axis and the magnetic field ( $|PA_{\text{outflow}} - \langle \Phi_B \rangle|$ ). Positive angles are measured from North (N) to East (E).

might show variability, we decided to add a sub-criterion: the selected sources should have had in 2011 a single-dish flux density greater than 20 Jy. This selection yielded 31 massive SFRs. One of these sources (Cepheus A) was actually observed by [24] with the Multi Element Remotely Linked Interferometer Network (MERLIN) in 2006. Therefore excluding this source and those already observed with the EVN, we observed a total number of 24 massive SFRs at 6.7 GHz from 2011 to 2015 (project codes: ES066, ES072).

### 3. Statistical Analysis

We detected linearly polarized emission of 6.7 GHz  $\text{CH}_3\text{OH}$  maser toward all the sources of the Flux-Limited sample but one, for a total of 233  $\text{CH}_3\text{OH}$  maser features, and circularly polarized emission toward 14 sources (33 maser features). We reported the detailed results of each source in a number of papers [1, 13–19]. To enlarge further the sample we also included in it all the massive YSOs of the southern hemisphere (declination  $< -9^\circ$ ) that were observed with an interferometer and that showed polarized 6.7 GHz  $\text{CH}_3\text{OH}$  maser emission. These are nine sources and they were all observed with the Australia Telescope Compact Array (ATCA) by [25]. The total number of sources toward which it was possible to measure the orientation of the magnetic field is 39, and for 27 of them we were able to compare the orientation of the magnetic field on the plane of the sky ( $\langle \Phi_B \rangle$ ) with the orientation of the outflows on the plane of the sky ( $PA_{\text{outflow}}$ ). In particular, we studied the statistical distribution of the angle between the outflow axis and the magnetic field ( $|PA_{\text{outflow}} - \langle \Phi_B \rangle|$ , see Fig. 1). First, we determined a probability of 2% that the distribution of the angles  $|PA_{\text{outflow}} - \langle \Phi_B \rangle|$  is drawn from a random distribution by performing a nonparametric Kolmogorov-Smirnov (K-S) test. This might suggest a preferred orientation of the magnetic field with respect to the outflow axis in massive YSOs. To verify this we performed two separated Monte Carlo simulation runs. One to determine the distribution on the plane of the sky of the angles if the outflow and the magnetic field are parallel in the 3D space (case 1, top left panel of Fig. 2) and the other one if they are perpendicular in the 3D space (case 2, top right panel of Fig. 2).

**Case 1.** The outflows have a certain opening angle, that conservatively can be assumed to be

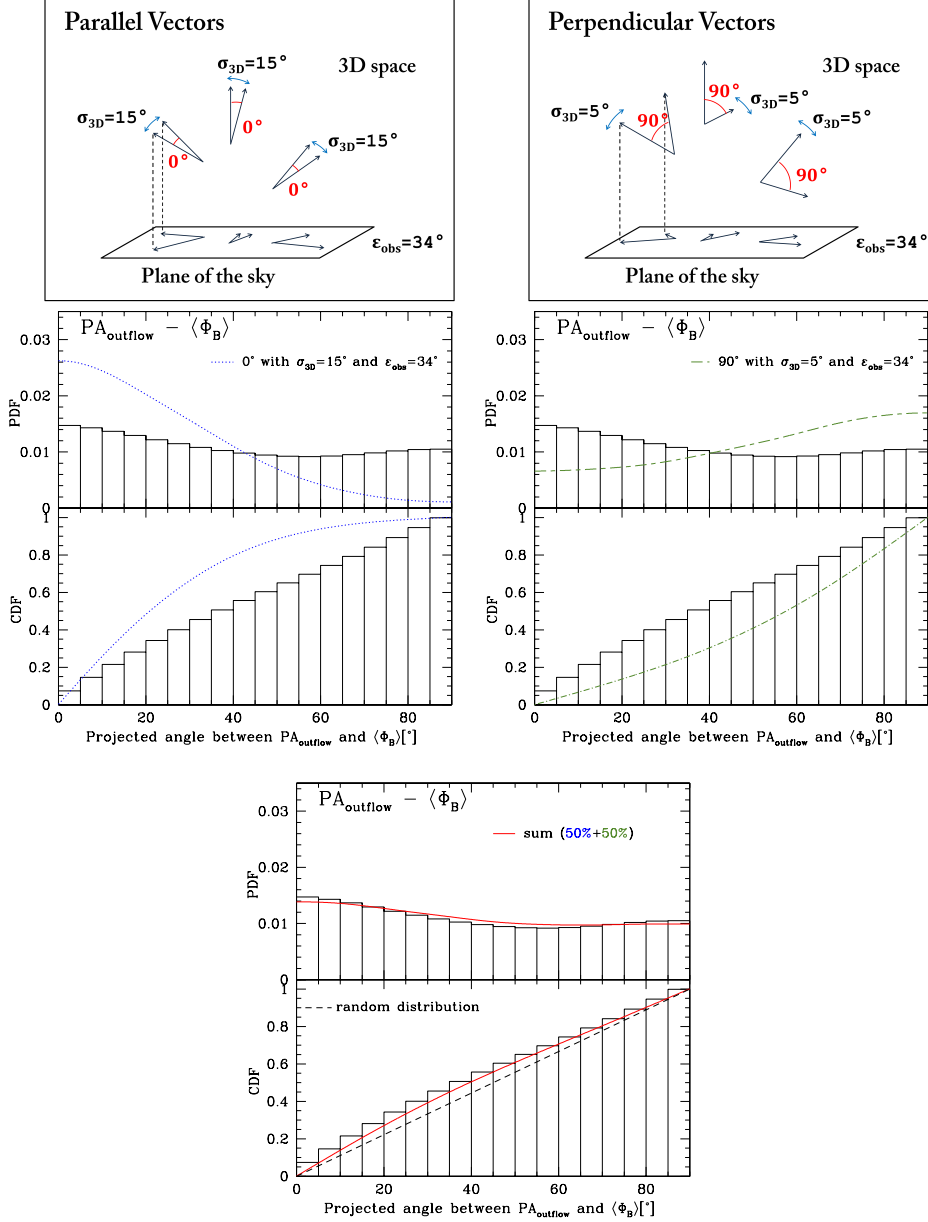


**Figure 2:** *Top panels:* Representation of the projected vectors on the plane of the sky of the random drawing, performed via Monte Carlo simulations, of parallel (left panel) and perpendicular (right panel) vectors (representing the outflow axes and the magnetic field) in the 3D space with a Gaussian uncertainty of  $15^\circ$  and  $5^\circ$ , respectively, and assuming a projected Gaussian error of  $34^\circ$ . *Middle panels:* Probability distribution function (PDF) and cumulative distribution function (CDF) of the projected angle between the magnetic field and the outflow axis ( $|PA_{\text{outflow}} - \langle \Phi_B \rangle|$ ). The dotted blue line and the dot-dashed green line are the results of the Monte Carlo simulations of the projection on the plane of the sky of two random 3D parallel vectors (left panel) and of two random 3D perpendicular vectors (right panel), respectively. *Bottom panel:* The red line is the best combination of the previous two Monte Carlo simulations to fit the observed data, each contributing for the 50%. The dashed black line is the CDF for completely random orientation of outflows and magnetic fields.

$30^\circ$ , therefore the magnetic field might be aligned either with the outflow axis (forming an angle of  $0^\circ$  with it) or with the edges of the outflow (forming an angle of  $15^\circ$  with the outflow axis). Consequently, in case 1 we decided to draw random vectors pairs that in the 3D space are parallel with a Gaussian sigma of  $15^\circ$ , furthermore their projection on the plane of the sky has an error equal to the median error that we measured in our sample, that is  $\varepsilon_{\text{obs}} = 34^\circ$ . The distribution of these projected angles is shown as a dotted blue line in the middle left panel of Fig. 2, where we compare it with the probability distribution function (PDF) and the cumulative distribution function (CDF) of the measured projected angle between the magnetic field and the outflow axis ( $|\text{PA}_{\text{outflow}} - \langle \Phi_{\text{B}} \rangle|$ ) of our sample.

**Case 2.** If the magnetic field is perpendicular to the outflow axis then the magnetic field is associated with a disk structure, which has some thickness. Therefore, we can expect that the magnetic field forms with the outflow axis an angle between  $85^\circ$  and  $95^\circ$ . Consequently, in case 2 we drew random vectors pairs that in the 3D space are perpendicular with a Gaussian sigma of  $5^\circ$  and their projection on the plane of the sky has an error of  $\varepsilon_{\text{obs}} = 34^\circ$ . We report the distribution of these projected angles as dot-dashed green line in the middle right panel of Fig. 2.

It is clear from Fig. 2 that we are not in any of the two studied cases. However, if we consider a combination of the two distributions (case 1 and case 2), we found that the best distribution that fits our observational data is the one where half of the sources is drawn from case 1 (parallel vectors in the 3D space) and half from case 2 (perpendicular vectors in the 3D space). This is shown as a solid red line in the bottom panel of Fig. 2, here we also show as dashed black line the CDF for completely random orientation of outflows and magnetic fields, i.e., all angular differences are equally likely. Therefore, it is clear that we have a perfect bimodal distribution that might be produced by the different evolutionary stages of the massive YSOs or might be due to where the 6.7 GHz  $\text{CH}_3\text{OH}$  masers arise in each source. Indeed, these masers are detected in the interface between the disk structure and the outflow of massive YSOs and then probing the magnetic field either associated with the disk structure or with the outflows.

### 3.1 Polarimetric characteristics of the 6.7 GHz $\text{CH}_3\text{OH}$ masers

We are able to determine the typical values of the linear ( $P_1$ ) and circular polarization fractions ( $P_V$ ) from the measurements of these quantities made toward the 6.7 GHz  $\text{CH}_3\text{OH}$  masers of the Flux-Limited sample. We show their PDF, along with that of the Zeeman-splitting of the maser line ( $\Delta V_Z$ ), in Fig. 3. A typical value for  $P_1$  (left panel in Fig. 3) is in the range  $P_1 = 1.0\% - 2.5\%$ , while for  $P_V$  we find that a typical value is in the range between  $0.5\%$  and  $0.75\%$  (middle panel). These ranges agree with the modeled values obtained by considering the cases where each of the eight hyperfine transitions, that might contribute to the 6.7 GHz  $\text{CH}_3\text{OH}$  maser emission, dominates the others and the special case where all these eight hyperfine transitions contribute equally [27]. However, it is not possible to determine the contribution of each hyperfine transition to the observed 6.7 GHz  $\text{CH}_3\text{OH}$  maser emission on the basis of the measured  $P_1$  and  $P_V$ . In addition of the measurements of  $P_V$ , we could also measure  $\Delta V_Z$  from the circularly polarized spectra. We note that typical values of  $\Delta V_Z$  are in the range between  $0.5 \text{ m s}^{-1}$  and  $2.0 \text{ m s}^{-1}$  (right panel of Fig. 3). This would correspond to a magnetic field strength along the line of sight of  $9 \text{ mG} < |B_{\parallel}| < 40 \text{ mG}$  if the dominating hyperfine transition is  $F = 3 \rightarrow 4$ .

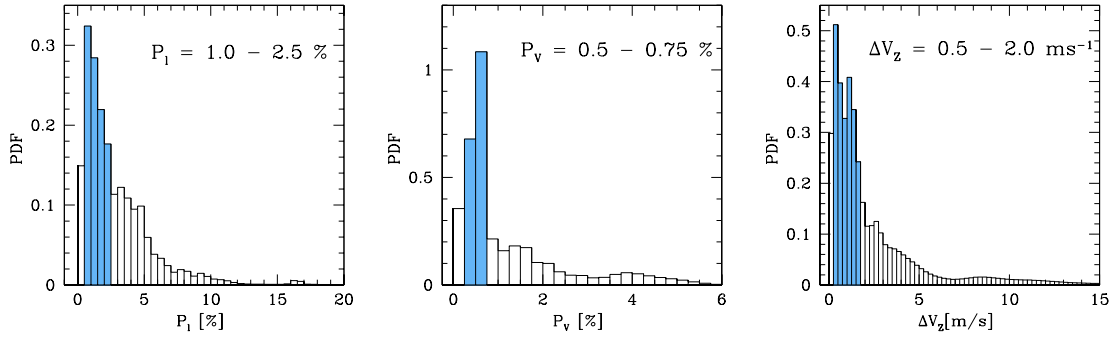


**Figure 3:** The PDF of the linear polarization fraction ( $P_1$ , *left panel*), of the circular polarization fraction ( $P_V$ , *middle panel*), and of the Zeeman-splitting ( $\Delta V_Z$ , *right panel*) of the 6.7 GHz  $\text{CH}_3\text{OH}$  maser emission. The interval width of the histograms is 0.5%, 0.25% and 0.25  $\text{m s}^{-1}$  for the  $P_1$ , the  $P_V$ , and the  $\Delta V_Z$  plots, respectively. Typical values of  $P_1$ ,  $P_V$ , and  $\Delta V_Z$  for the 6.7 GHz  $\text{CH}_3\text{OH}$  maser emission is highlighted in blue. The data are taken from [1, 13, 14, 16–19, 24, 26].

## References

- [1] G. Surcis, W.H.T. Vlemmings, H.J. van Langevelde, B. Hutawarakorn Kramer and A. Bartkiewicz, *EVN observations of 6.7 GHz methanol maser polarization in massive star-forming regions. V. Completion of the flux-limited sample*, *A&A* **658** (2022) A78 [2111.08023].
- [2] A. Frank, T.P. Ray, S. Cabrit, P. Hartigan, H.G. Arce, F. Bacciotti et al., *Jets and Outflows from Star to Cloud: Observations Confront Theory*, in *Protostars and Planets VI*, H. Beuther, R.S. Klessen, C.P. Dullemond and T. Henning, eds., p. 451, Jan., 2014, DOI [1402.3553].
- [3] J. Bally, *Protostellar Outflows*, *ARA&A* **54** (2016) 491.
- [4] G. Anglada, L.F. Rodríguez and C. Carrasco-González, *Radio jets from young stellar objects*, *A&ARv* **26** (2018) 3 [1806.06444].
- [5] T.P. Ray and J. Ferreira, *Jets from young stars*, *New Astron. Rev.* **93** (2021) 101615 [2009.00547].
- [6] R.E. Pudritz and T.P. Ray, *The Role of Magnetic Fields in Protostellar Outflows and Star Formation*, *Frontiers in Astronomy and Space Sciences* **6** (2019) 54 [1912.05605].
- [7] P. Hennebelle, B. Commerçon, M. Joos, R.S. Klessen, M. Krumholz, J.C. Tan et al., *Collapse, outflows and fragmentation of massive, turbulent and magnetized prestellar barotropic cores*, *A&A* **528** (2011) A72 [1101.1574].
- [8] D. Seifried, R.E. Pudritz, R. Banerjee, D. Duffin and R.S. Klessen, *Magnetic fields during the early stages of massive star formation - II. A generalized outflow criterion*, *MNRAS* **422** (2012) 347 [1109.4379].

- [9] R. Banerjee and R.E. Pudritz, *Massive Star Formation via High Accretion Rates and Early Disk-driven Outflows*, *ApJ* **660** (2007) 479 [[astro-ph/0612674](#)].
- [10] A.L. Rosen and M.R. Krumholz, *The Role of Outflows, Radiation Pressure, and Magnetic Fields in Massive Star Formation*, *AJ* **160** (2020) 78 [[2006.04829](#)].
- [11] C.L.H. Hull and Q. Zhang, *Interferometric observations of magnetic fields in forming stars*, *Frontiers in Astronomy and Space Sciences* **6** (2019) 3 [[1903.03177](#)].
- [12] Q. Zhang, K. Qiu, J.M. Girart, H.B. Liu, Y.-W. Tang, P.M. Koch et al., *Magnetic Fields and Massive Star Formation*, *ApJ* **792** (2014) 116 [[1407.3984](#)].
- [13] G. Surcis, W.H.T. Vlemmings, R. Dodson and H.J. van Langevelde, *Methanol masers probing the ordered magnetic field of W75N*, *A&A* **506** (2009) 757 [[0908.3585](#)].
- [14] G. Surcis, W.H.T. Vlemmings, R.M. Torres, H.J. van Langevelde and B. Hutawarakorn Kramer, *The properties and polarization of the H<sub>2</sub>O and CH<sub>3</sub>OH maser environment of NGC 7538-IRS 1*, *A&A* **533** (2011) A47 [[1107.5313](#)].
- [15] G. Surcis, W.H.T. Vlemmings, H.J. van Langevelde and B. Hutawarakorn Kramer, *EVN observations of 6.7 GHz methanol maser polarization in massive star-forming regions*, *A&A* **541** (2012) A47 [[1203.4566](#)].
- [16] G. Surcis, W.H.T. Vlemmings, H.J. van Langevelde, B. Hutawarakorn Kramer and L.H. Quiroga-Nuñez, *EVN observations of 6.7 GHz methanol maser polarization in massive star-forming regions. II. First statistical results*, *A&A* **556** (2013) A73 [[1306.6335](#)].
- [17] G. Surcis, W.H.T. Vlemmings, H.J. van Langevelde, L. Moscadelli and B. Hutawarakorn Kramer, *The magnetic field at milliarcsecond resolution around IRAS 20126+4104*, *A&A* **563** (2014) A30 [[1401.7987](#)].
- [18] G. Surcis, W.H.T. Vlemmings, H.J. van Langevelde, B. Hutawarakorn Kramer, A. Bartkiewicz and M.G. Blasi, *EVN observations of 6.7 GHz methanol maser polarization in massive star-forming regions. III. The flux-limited sample*, *A&A* **578** (2015) A102 [[1504.06325](#)].
- [19] G. Surcis, W.H.T. Vlemmings, H.J. van Langevelde, B. Hutawarakorn Kramer and A. Bartkiewicz, *EVN observations of 6.7 GHz methanol maser polarization in massive star-forming regions. IV. Magnetic field strength limits and structure for seven additional sources*, *A&A* **623** (2019) A130 [[1902.08210](#)].
- [20] G. Surcis, W.H.T. Vlemmings, H.J. van Langevelde and B. Hutawarakorn Kramer, *High resolution magnetic field measurements in high-mass star-forming regions using masers*, in *Proceedings of the 11th European VLBI Network Symposium & Users Meeting. 9-12 October*, p. 34, Oct., 2012, DOI.
- [21] G. Surcis, W.H.T. Vlemmings, H.J. van Langevelde, B. Hutawarakorn Kramer, A. Bartkiewicz and H. Engelkamp, *Magnetic field measurements at milliarcsecond*

- resolution around massive young stellar objects.*, in *Proceedings of the 12th European VLBI Network Symposium and Users Meeting (EVN 2014)*. 7-10 October 2014. Cagliari, p. 41, Jan., 2014, [DOI](#).
- [22] G. Surcis, W.H.T. Vlemmings and H. Van Langevelde, *Magnetic field measurements around massive young stellar objects with the EVN.*, in *14th European VLBI Network Symposium & Users Meeting (EVN 2018)*, p. 3, Nov., 2018, [DOI](#).
- [23] M.R. Pestalozzi, V. Minier and R.S. Booth, *A general catalogue of 6.7-GHz methanol masers. I. Data.*, *A&A* **432** (2005) 737 [[astro-ph/0411564](#)].
- [24] W.H.T. Vlemmings, G. Surcis, K.J.E. Torstensson and H.J. van Langevelde, *Magnetic field regulated infall on the disc around the massive protostar CepheusAHW2*, *MNRAS* **404** (2010) 134 [[1002.2214](#)].
- [25] R. Dodson and C.D. Moriarty, *Probing the magnetic fields of massive star-forming regions with methanol maser polarization*, *MNRAS* **421** (2012) 2395 [[1201.1687](#)].
- [26] G. Surcis, W.H.T. Vlemmings, S. Curiel, B. Hutawarakorn Kramer, J.M. Torrelles and A.P. Sarma, *The structure of the magnetic field in the massive star-forming region W75N*, *A&A* **527** (2011) A48 [[1101.1956](#)].
- [27] D. Dall’Olio, W.H.T. Vlemmings, B. Lankhaar and G. Surcis, *Polarisation properties of methanol masers*, *A&A* **644** (2020) A122 [[2010.04737](#)].